# NEW MINIMAL SURFACES IN $S^3$

H. Karcher, U. Pinkall and I. Sterling

Max-Planck-Institut für Mathematik
Gottfried-Claren-Str. 26
5300 Bonn 3

MPI 86-27

# NEW MINIMAL SURFACES IN $S^3$

H. Karcher, U. Pinkall and I. Sterling

Abstract

In this paper we construct new examples of compact imbedded minimal surfaces in $S^3$. We show some of these provide counterexamples to the conjecture that imbedded minimal surfaces separate $S^3$ into two domains of equal volume.

## 1. Introduction

We begin with the well-known tessellations of $S^3$ into cells having the symmetry of a Platonic solid in $\mathbb{R}^3$ and dihedral angle $2\beta_1$. Dividing a cell by its planes of symmetry we obtain as a fundamental region for the group of symmetries a tetrahedron with dihedral angles $\pi/2,\ \pi/2,\ \pi/2,\ \eta,\ \beta_1,\ \beta_2$. (See Table 1). The tetrahedron is determined by its dihedral angles.

Table 1

| $\eta,\beta_1,\beta_2$ | Cell Type | # of cells in tessellation | genus of constructed surfaces |
|---|---|---|---|
| $\pi/3,\pi/3,\pi/3$ | Tetrahedral (Self-Dual) | 5 | 6 |
| $\pi/4,\pi/3,\pi/3$ | Octahedral (Self-Dual) | 24 | 73 |
| $\pi/3,\pi/3,\pi/4$ | Tetrahedral (or Cubical) | 16 (or 8) | 17 |
| $\pi/3,\pi/3,\pi/5$ | Tetrahedral (or Dodecahedral) | 600 (or 120) | 601 |
| $\pi/3,\pi/2,\pi/3$ | Tetrahedral | 2 | 3 |
| $\pi/3,\pi/2,\pi/4$ | Cubical | 2 | 5 |
| $\pi/3,\pi/2,\pi/5$ | Dodecahedral | 2 | 11 |
| $\pi/4,\pi/2,\pi/3$ | Octahedral | 2 | 7 |
| $\pi/5,\pi/2,\pi/3$ | Isocahedral | 2 | 19 |

To construct a minimal surface in $S^3$, we first find a minimal surface with boundary, called a "patch", within a tetrahedron (from Table 1) which intersects orthogonally all the plane-faces of the tetrahedron in planar geodesics. From the patch we obtain a certain piece of the whole surface, called a "bone", by repeatedly reflecting "patches" through those plane-faces of the tetrahedron which are not contained in faces of the cell. Finally, we build the complete surface using reflections through faces of the cells. (See Figs. 1-3).

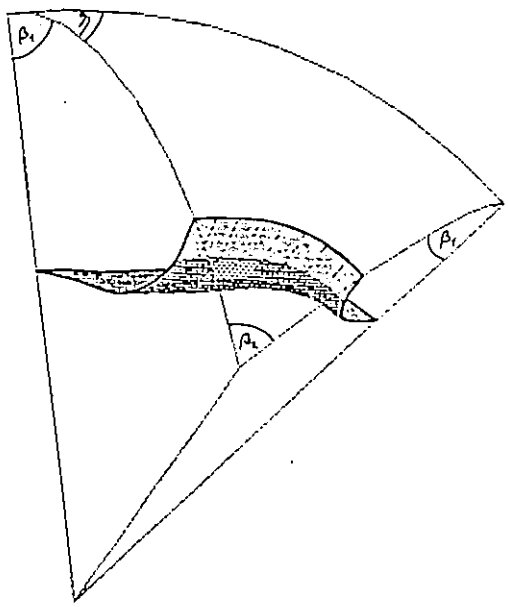

Figure 1

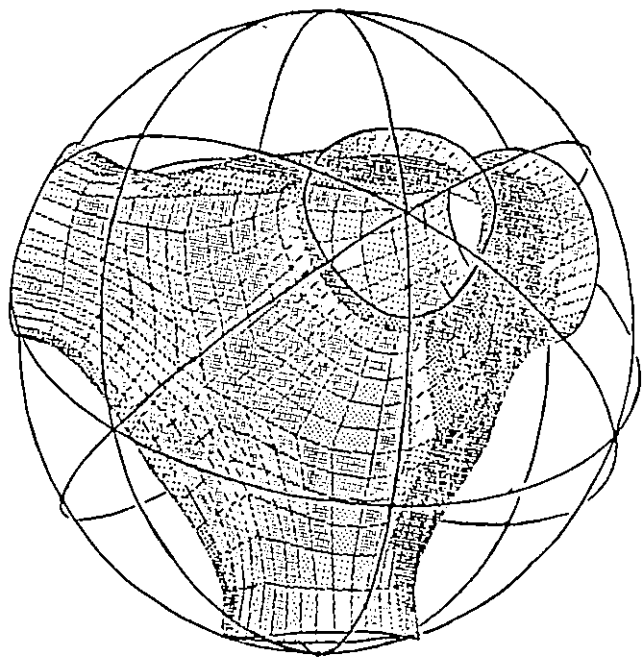

Figure 2

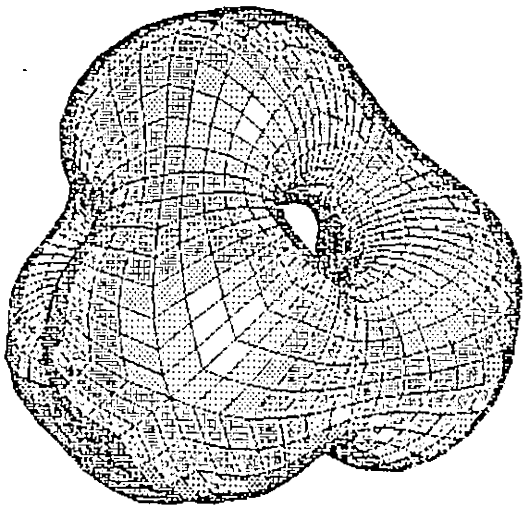

Figure 3

In § 2 we outline our strategy of constructing the mentioned "patch". A similar construction has been used to obtain complete minimal surfaces in $\mathbb{R}^3$ [5,p. 66, 6] but in $S^3$ the arguments are more involved. The necessary control over the construction comes from lemmas based on the maximum principle (§ 3). This is enough to prove existence (§4). In §5 we get sufficient control on the polar minimal surface to prove that the "patch" is a graph in polar coordinates as in Figure 1; this implies imbeddedness.

Such imbedded minimal surfaces divide $S^3$ into two components whose volumes were conjectured to be always equal [7]. We have enough control on our surfaces to ensure in § 5 that for some of them these two volumes are different.

For self-dual tessellations there is a simpler construction. In the case $(\pi/3,\pi/3,\pi/3)$

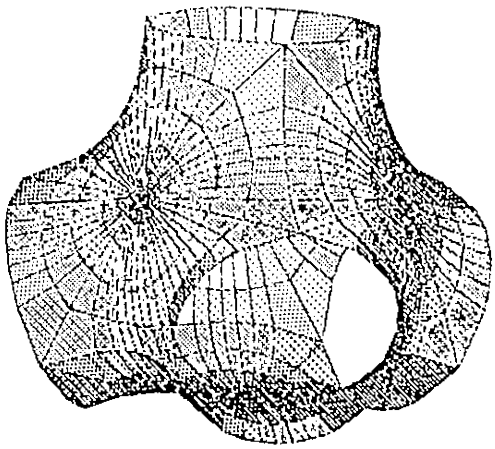

Figure 4

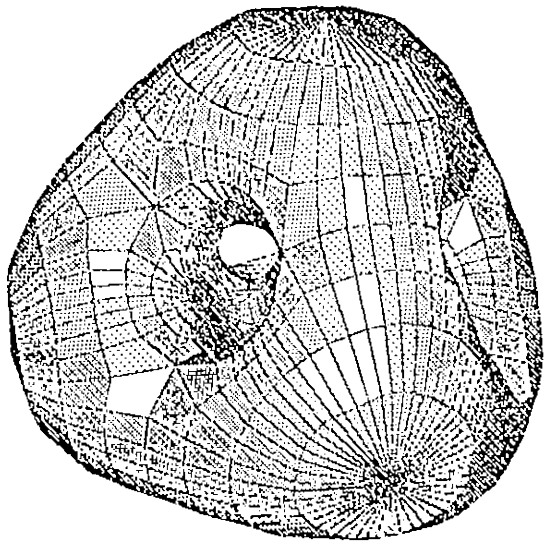

Figure 5

(resp. $(\pi/4,\pi/3,\pi/3)$) one solves the Plateau problem for the geodesic quadrilateral with all lengths $\pi/4$ (resp. $\pi/8$) and opposite angles equal $\pi/2$, $\pi/3$ (resp. $\pi/2,\pi/4$). Repeated reflections through the boundary geodesics directly yield the entire surface. One fifth (resp. one $24^{th}$) of this surface is a "bone" with boundary on a tetrahedral (resp. octahedral) cell. (see Figs. 4-5).

These simpler examples do seperate $S^3$ into two components of equal volume. Indeed, the fact that these surfaces contain great circles implies that they separate $S^3$ into congruent components.

## 2. Outline of construction

We assume the results of [3,4]. Whenever necessary, $\eta$ is fixed.

We want to find a minimal surface, in the fundamental tetrahedron, intersecting all faces perpendicularly and meeting those edges which have dihedral angles $\pi/2,\pi/2,\pi/2,\eta$. Such a patch is conjugate to a minimal surface bounded by a geodesic qudrilateral ABCD with angles $\pi/2,\pi/2,\pi/2,\eta$ at A,B,C,D. Such quadrilaterals have two free parameters, e.g. the edgelengths $\ell_1,\ell_2$ at A. The other two edge lengths $S_1,S_2$ are determined by $\cos S_1 \cos \ell_1 = \cos S_2 \cos \ell_2$ and $\cos \ell_1 \cos \ell_2 = \cos S_1 \cos S_2 + \sin S_1 \sin S_2 \cos \eta$. (See Fig. 6).

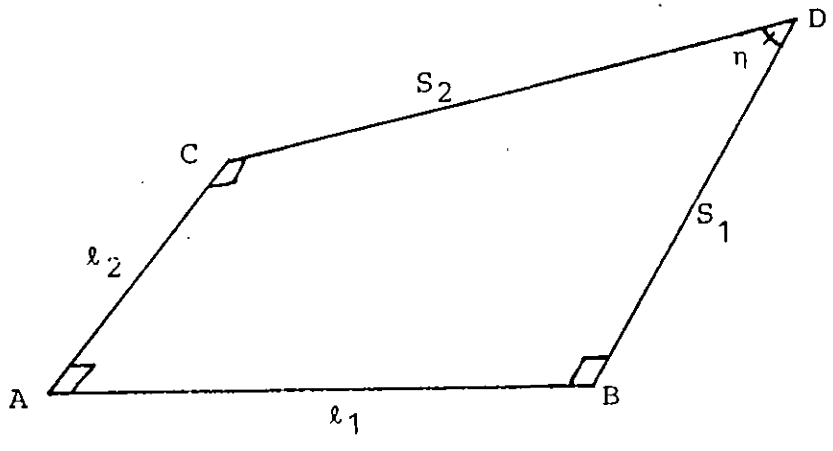


Figure 6

Let $M(\eta,\ell_1,\ell_2)$ denote the unique (§3) Plateau solution for any such geodesic quadrilateral. The conjugate minimal surface, denoted $M^*(\eta,\ell_1,\ell_2)$, determines by its planar boundary arcs a tetrahedron having, at the vertices $A^*,B^*,C^*,D^*$ of this "patch", dihedral angles $\pi/2,\pi/2,\pi/2,\eta$. We have to choose $\ell_1,\ell_2$ in such a way that the other two dihedral angles are $\beta_1,\beta_2$ from Table 1. These dihedral angles are given as the angles between the normal planes at the endpoints of the (spherically) planar curves $\ell_1^*$ resp. $\ell_2^*$. These curves are determined by their geodesic curvature function $\kappa_i(\eta,\ell_1,\ell_2)$ $(i = 1,2)$. We denote by $\alpha_i(\eta,\ell_1,\ell_2)$ the functions $\alpha_i(u)$ which gives the turning angle between the totally geodesic plane through $ABC$ and the tangent plane of $M(\eta,\ell_1,\ell_2)$ at the point on $\ell_i$ which has distance $u$ from $A$. Then $\kappa_i = \alpha_i'$ [3, p. 368].

In this way the dihedral angles $\beta_1,\beta_2$ are determined by the geodesic quadrilateral $Q = Q(\eta,\ell_1,\ell_2)$. Note

Note $\cos\alpha_1(B) = \frac{\cos\ell_2\cdot\tan\ell_1}{\tan S_1} > 0$, $\cos\alpha_2(C) = \frac{\cos\ell_1\cdot\tan\ell_2}{\tan S_2} > 0$.

From [4,Thm. 2] and from the argument [3,p. 350] we have

Lemma 1. The Plateau solution $M(\eta,\ell_1,\ell_2)$ is contained in the convex hull $C(Q)$ of the boundary quadrilateral. The intrinsic curvature of $M$ is less than 1, except at $D$; therefore, all the turning angle functions of the four edges are strictly monotone. Hence, also, $\ell_1^*,\ell_2^*,S_1^*,S_2^*$ are locally convex. □

The Frenet frame $x,t,n$ of the curve $\ell_i^*$ is controlled by the Frenet equations

$$(1)\qquad \begin{cases} x' = t \\ t' = -x + \kappa n \\ r' = -\kappa t \end{cases} \quad \text{or} \quad \begin{cases} x' = a \cdot \cos\alpha + b \sin\alpha \\ a' = -x \cdot \cos\alpha \\ b' = -x \cdot \sin\alpha \end{cases}$$

where $\alpha = \alpha_i(\eta,\ell_1,\ell_2)$, $\kappa = \alpha'$, $a = t\cdot\cos\alpha - n\cdot\sin\alpha$, $b = t\cdot\sin\alpha + n\cdot\cos\alpha$. Observe $\beta_i = \cos^{-1} \langle t(\ell_i), t(0)\rangle$.

The second version of the Frenet equations does not need the derivative of the turning angle function $\alpha$. This will allow us to prove continuity of the map $(\beta_1,\beta_2) := F_\eta(\ell_1,\ell_2)$ and to establish sufficiently narrow bounds which imply that the $(\beta_1,\beta_2)$-pairs of Table 1 are in the range of $F_\eta$ - thus establishing existence of all the patches.

## 3. The maximum principle and basic lemmas

Maximum principle [5]. Suppose that $M_1, M_2$ are two branched minimal surfaces such that for a point $p \in M_1 \cap M_2$ the surface $M_1$ locally lies on one side of $M_2$ near $p$. Then the surfaces $M_1, M_2$ coincide near $p$.

We have already quoted from Lawson [4], that a minimal surface contained in an open half sphere actually is contained in the convex hull of its boundary - because, for equator spheres $S$, it is clear what is meant by "M lies on one side of $S$". We wish to use the following ruled minimal surfaces ("helicoids") as comparison surfaces in the maximum principle.

A helicoid with constant turning speed $\tau$ is given as follows: let $c(s)$ be a geodesic (called an axis) and $e_1(s)$, $e_2(s)$ orthonormal parallel fields along $c$. Then $H(s,t) := \exp_{c(s)} t \cdot (e_1(s) \cos(\tau \cdot s) + e_2(s) \cdot \sin(\tau \cdot s))$, $(0 \leq s \leq \ell,\ 0 \leq t \leq \frac{\pi}{2})$. The tangent turning angle along the rulings is not constant, but is given by $\tan \alpha(t) = \tau \cdot \tan t$. ($\tau = 1$ gives the Clifford torus, $\tau = 2$ Lawson's Klein bottle.)

The orbits of the rotation around $c$ are transversal to the helicoid except on $c$ and its polar circle. We will choose helicoids having as an axis one of the edges $\ell_1, \ell_2$ of the quadrilateral $Q$ and with the property that the convex hull $C(Q)$ can be rotated around the axis to a position where it meets the helicoid only along the axis.

Then we have an:

Extended maximum principle. If one rotates the Plateau solution, $M$, of $Q$ in either direction around the axis, then $M$ first meets the helicoid (excluding the axis) at a boundary point. (This is also true in euclidean geometry.)

The same sort of "extended maximum principle" will be applied below also to other comparison surfaces than helicoids.

Proof. Directly by the maximum principle the helicoid and $M$ cannot first meet at an interior point. We have to exclude the case that the Plateau solution first becomes tangential to the helicoid at interior points of the axis and not at the end-points. To do so we choose an auxiliary axis $\bar{c}$ in such a common tangent plane by extending the touching ruling to $t = -\varepsilon$ and choose $\bar{c}$ perpendicular to the rule. Now continue the rotation of $M$ around $c$ a little further and rotate back around $\bar{c}$. In this way the Plateau solution can be moved to touch the helicoid from one side at an interior point -a contradiction.

□

There is an optimal choice of such comparison helicoids due to the following: If one describes the edge $S_1$ (resp. $S_2$) in helicoidal coordinates with axis $\ell_2$ (resp. $\ell_1$) one finds convex turning angle functions $\tilde{\alpha}(u)$ given by

$$\tan \tilde{\alpha}(u) = \frac{\tan \alpha(\ell)}{\tan \ell} \cdot \tan u, \quad 0 \leq u \leq \ell \quad \text{(note: } \ell_i < \alpha(\ell_i) < \tfrac{\pi}{2}\text{)}.$$

The secant of $\tilde{\alpha}(u)$ has slope $\underline{\tau} = \frac{\alpha(\ell)}{\ell}$, the initial tangent of $\tilde{\alpha}(u)$ has slope $\overline{\tau} = \frac{\tan \alpha(\ell)}{\tan \ell}$. These are the optimal constant turning speeds for helicoids (axis $\ell_i$) which touch the quadrilateral from one side or from the other. Because of our extended maximum principle, they leave the Plateau solution on one side. Our notations are such that $\alpha_2$ is increasing, and $\alpha_1$ is decreasing. We therefore get lower bounds for $\alpha_2$ (resp. $-\alpha_1$) from the two helicoids with axis $\ell_i$ and turning speed $\underline{\tau}_i$, and upper bounds with $\overline{\tau}_i$ $(i = 1,2)$.

$$
(2) \qquad \begin{cases} \alpha_2^{1L}(u) = \tan^{-1}(\underline{\tau}_1 \cdot \tan u) \\ \alpha_2^{2L}(u) = \underline{\tau}_2 \cdot u \quad \text{(the secant of the function } \alpha_2\text{)} \\ \alpha_2^{1U}(u) = \tan^{-1}(\overline{\tau}_2 \tan u) \\ \alpha_2^{1U}(u) = \overline{\tau}_1 \cdot u \quad \text{(the initial tangent of } \alpha_2\text{)} \\ \text{similar formulas hold along } \ell_1 . \end{cases}
$$

We summarize this as

Lemma 2. $\alpha_i^{jL}(u) \leq \alpha_i(u) \leq \alpha_i^{jU}(u)$, $0 \leq u \leq \ell_i$ $(i,j = 1,2)$. □

Lemma 3. Any minimal surface with boundary $Q$ and in the convex hull of $Q$ is the unique Plateau solution.

Proof. Since $Q$ has geodesic edges, we can extend the minimal surfaces by 180°-rotation to a rim around the quadrilateral. Since the turning angles $\alpha_i$ are less than

$\pi/2$ one can rotate a second copy of the convex hull by 180° around $\ell_i$ so that the two copies meet only along the edge $\ell_i$. Having two different minimal surfaces bounding Q and in the convex hull clearly contradict our extension of the maximum principle.

□

Lemma 4. The function $(\beta_1, \beta_2) = F_\eta(\ell_1, \ell_2)$ is continuous.

Proof. Given $\varepsilon$ we rotate Q around $\ell_1$ (resp. $\ell_2$) by $\varepsilon$. A sufficiently small change of $\ell_1, \ell_2$ in the rotated position will leave the changed quadrilateral on one side of M. Again, by the extended maximum principle, this proves that the new turning functions are in an $\varepsilon$-strip around the initial $\alpha_i$'s. The second version of the Frenet equations now shows that the $\beta_i$'s change correspondingly little.

□

## §4 Existence

Lemma 5. Let $s \longmapsto x(s)$, $s \longmapsto \underline{x}(s)$, and $s \longmapsto \overline{x}(s)$, $0 \leq s \leq \ell$ be three locally convex arcs on $S^2$, of the same length $\ell < \frac{\pi}{2}$. Let $\kappa, \underline{\kappa}$ and $\overline{\kappa}$ denote the corresponding geodesic curvatures, $(x,t,n)$, $(\underline{x},\underline{t},\underline{n})$, and $(\overline{x},\overline{t},\overline{n})$ the corresponding Frenet-frames with $\det(x,t,n) = 1$, $\underline{\alpha}(u) = \int_0^u \underline{\kappa}(s)ds$ the integrated curvatures, etc. Assume for all $s$

$$\underline{\alpha}(s) \leq \alpha(s) \leq \overline{\alpha}(s) < \frac{\pi}{2} . \tag{3}$$

Then

a) $\langle \underline{x}(s), \underline{t}(0) \rangle \geq \langle x(s), t(0) \rangle \geq \langle \overline{x}(s), \overline{t}(0) \rangle$ for all $s$,

b) $\cos \alpha(\ell) - \int_0^\ell \cos((\alpha/\ell) - \overline{\alpha}) \langle \underline{x}(s)\overline{t}, t(0) \rangle ds$

$$\leq \langle t(\ell), t(0) \rangle$$

$$\leq \cos \alpha(\ell) - \int_0^\ell \cos(\alpha(\ell) - \underline{\alpha}) \langle \overline{x}(s), \overline{t}(0) \rangle ds.$$

Proof. b) follows easily from (1), (3) and a) by using $-(\cos \alpha(\ell) \cos \alpha + \sin \alpha(\ell) \sin \alpha) = -\cos(\alpha(\ell) - \alpha) \leq -\cos(\alpha(\ell) - \underline{\alpha})$, etc. To prove a) we first show

$$\begin{array}{lll} \langle x(s), x(0) \rangle > 0 & \langle t(s), x(0) \rangle < 0 & \langle n(s), x(0) \rangle > 0 \\ \langle x(s), t(0) \rangle > 0 & & \langle n(s), t(0) \rangle < 0 \\ \langle x(s), n(0) \rangle > 0 & \langle t(s), n(0) \rangle > 0 & \langle n(s), n(0) \rangle > 0 \\ \langle x(s) \times x(t), t(0) \rangle > 0 \quad \text{for} \quad t > s. & & \text{(See Fig. 7).} \end{array} \tag{4}$$

Remark. These inequality imply x and n are convex (not only locally convex.)

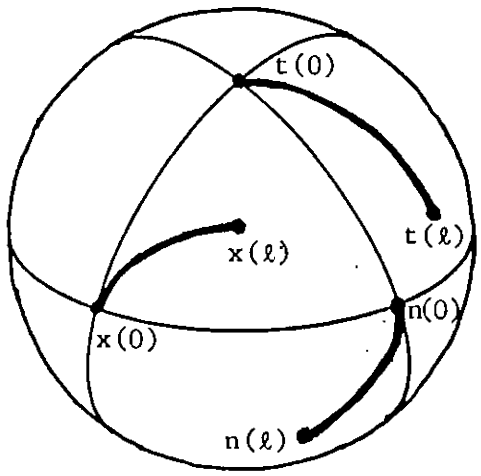


Figure 7

By the Frenet equations, (4) clearly holds for small $s > 0$. It is therefore sufficient to see that none of the scalar products in (4) can become zero for $s > 0$. In the cases $\langle x(s),x(0)\rangle$ and $\langle n(s),n(0)\rangle$, this follows from the fact that the curves x and n have lengths $\ell$ and $\alpha(\ell)$ respectively, both being less than $\pi/2$.

The tangent great circle of the curve x never passes through the point $n(0)$, because then we would have $\langle n(s),n(0)\rangle = 0$. This together with the local convexity of x implies all our inequality (4) involving $t(s)$. A similar argument (note that also n is a locally convex

curve with curvature $\frac{1}{\kappa}$) implies the assertions in (14) about $n(s)$.

The geodesic segment from $x(s)$ to $n(s)$ cuts the great circle polar to $t(0)$ in a point $y$ satisfying $\langle y, x(0)\rangle > 0$, $\langle y, n(0)\rangle > 0$. This implies our claims about $t(s) = x(s) \times n(s)$, proving all of (4) (and the remark following (4)).

Secondly, given $\varepsilon > 0$, one may choose step functions $\underline{\alpha}, \tilde{\alpha}$ such that

$$\alpha(s) - \varepsilon \leq \underline{\alpha}(s) \leq \alpha(s) \leq \tilde{\alpha}(s) \leq \alpha(s) + \varepsilon \ . \tag{5}$$

The corresponding $\tilde{x}, \underline{x}$ given by the second version of the Frenet equations (1) are then close to $x$ in the sense that $\lim_{\varepsilon \to 0} \tilde{x}, \underline{x} = x$.

Therefore it suffices to prove a) for the case where $\underline{x}$, $x$, and $\bar{x}$ are all polygons. We work now with $\bar{x}$ and $x$, the case of $x$ and $\underline{x}$ is similar. By subdividing we can assume that the vertices of $x$ and $\bar{x}$ correspond to the same parameter values $0 = s_n < s_{n-1} < \ldots s_1 < s_0 = \ell$. We define a one-parameter family of polygons $x_\lambda$, $0 \leq \lambda \leq n$, $x_0 = x$, $x_n = \bar{x}$ corresponding to the integrated curvature functions $\alpha_\lambda$ defined inductively on $v$ as follows: $\alpha_0 = \alpha$ and for $\lambda = v + d$, $v \in \{0, \ldots, n-1\}$, $0 < d \leq 1$, we set

$$(6)\qquad \alpha_\lambda(s) = \begin{cases} \alpha_\nu(s) & \text{for } s \notin (s_{\nu+1}, s_\nu] \\ (1-d)\,\alpha_\nu(s) + d\bar{\alpha}(s) & \text{for } s \in (s_{\nu+1}, s_\nu] \end{cases} .$$

All $\alpha_\lambda$ are non-decreasing, so the polygons $x_\lambda$ are convex, and hence the inequalities (4) are available for $x_\lambda$. To compare polygons for different $\lambda$, we assume, with the obvious notation,

$$(7)\qquad \begin{aligned} x_\lambda(0) &= x(0), \\ t_\lambda(0) &= t(0), \\ n_\lambda(0) &= n(0), \end{aligned}$$

for all $\lambda$. Using this we will prove

$$(8)\qquad \frac{d}{d\lambda} \langle x_\lambda(s), t(0) \rangle \le 0, \quad \text{for } \lambda \notin \mathbb{Z},$$

and for every fixed $s$. This, obviously, will complete the proof.

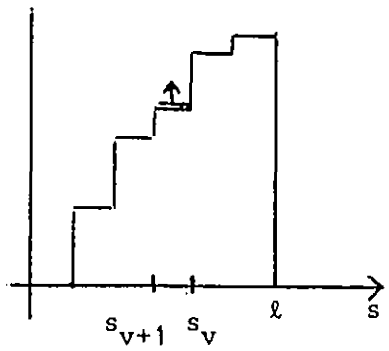


Figure 8

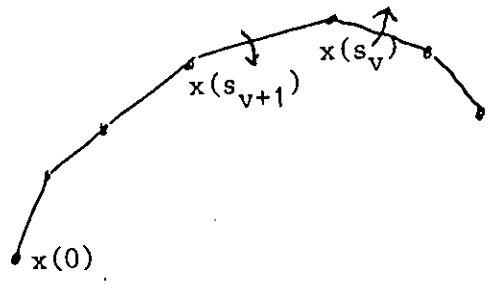


Figure 9

(6) means that the function $\alpha_\lambda$ is fixed except on the interval $(s_{v+1}, s_v]$ where it is moving upward at a constant speed. (See Figs. 8-9). For the corresponding polygon $x_\lambda$, this means that the angle at the vertex $x(v)$ is increasing at a certain rate, while the angle at $x(v+1)$ is decreasing at the same rate.

Clearly then, the last inequality (4) implies (8) for $s \in (v, v+1]$; and thus (since points $x_\lambda(s)$ for $s \leq s_v$ are not moving at all) for $s \leq s_{v+1}$. The increasing kink at $x_\lambda(s_v)$ imposes on all $x_\lambda(s)$, $s > s_v$, an infinitesimal rotation with angular velocity vector $\omega = -c\, x_\lambda(s_v)$ for some constant $c > 0$. The decreasing kink at $x_\lambda(s_{v+1})$ induces a rotation with $\omega = c x_\lambda(s_{v+1})$. The linearity of the Frenet equations implies that the total effect on $x_\lambda(s)$, $s > s_{v+1}$ is an infinitesimal rotation with angular velocity

(a) $$w = c(x_\lambda(s_{v+1}) - x_\lambda(s_v)) = \tilde{c}\, t_\lambda(s) \quad \text{for some } s \in (s_{v+1}, s_v]$$

$\tilde{c} > 0$ together with the information in (4) then yields (8). □

Theorem. The minimal surfaces listed in Table 1 exist; more specifically: for all $\eta, \beta_1, \beta_2$ of Table 1 there exist $(\ell_1, \ell_2)$ such that $F_\eta(\ell_1, \ell_2) = (\beta_1, \beta_2)$.

Proof. The idea is to find a contractible curve $\ell(s) = (\ell_1(s), \ell_2(s))$ such that the curve $F_\eta(\ell(s))$ has nonzero winding number around the point $(\beta_1, \beta_2)$ (See Figs. 10-11).

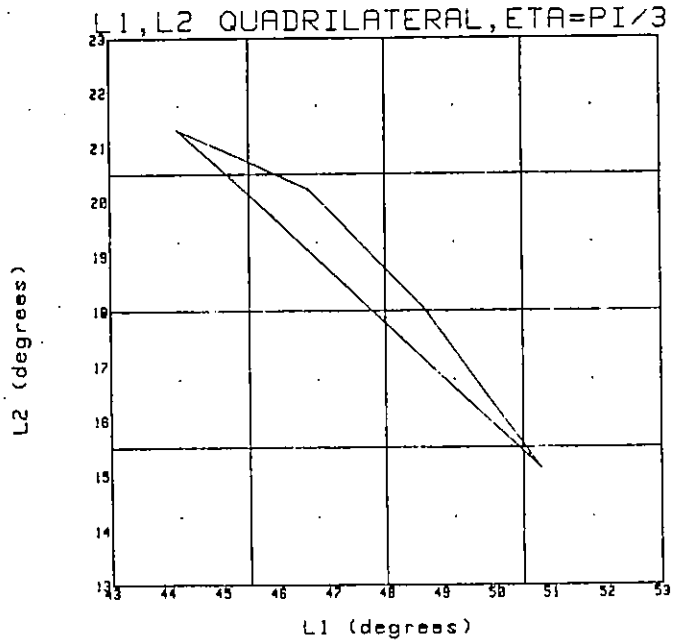


Figure 10

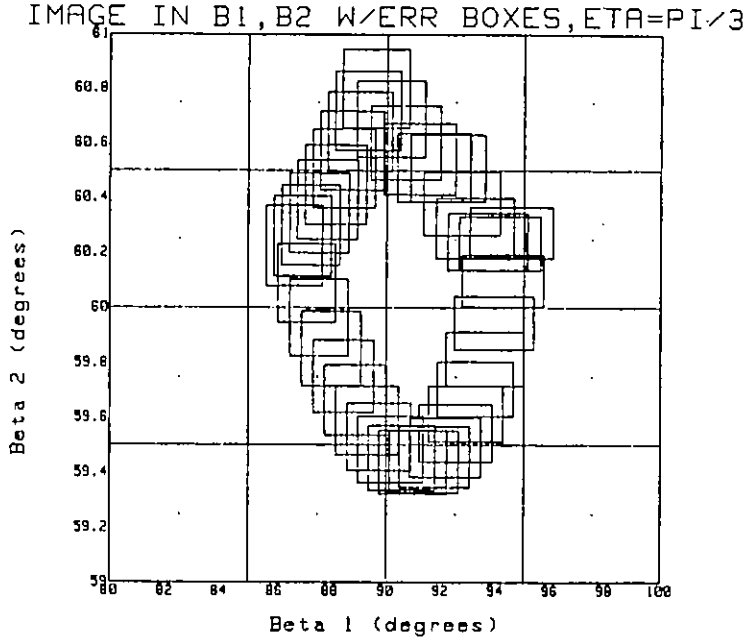


Figure 11

This is easy for the third and fourth examples of Table 1: (See Fig. 12) Along $\cos \ell_1 \cos \ell_2 = \cos \eta$ we have $\pi/2 = \alpha_i \leq \beta_i$ $(i = 1,2)$. Along the other three parts we have $\lim_{\epsilon \to 0} \beta_i = \alpha_i$ ; the small circle corresponds to the euclidean limit where $\cos \eta = \sin \alpha_1 \cdot \sin \alpha_2$, and on the two straight portions we have: $\ell_2 \to 0$ (resp. $\ell_1 \to 0$) implies $\alpha_1 \to \pi/2$ (resp. $\alpha_2 \to \pi/2$). (This also works for the first and second examples of Table 1 which were discussed separately in § 1).

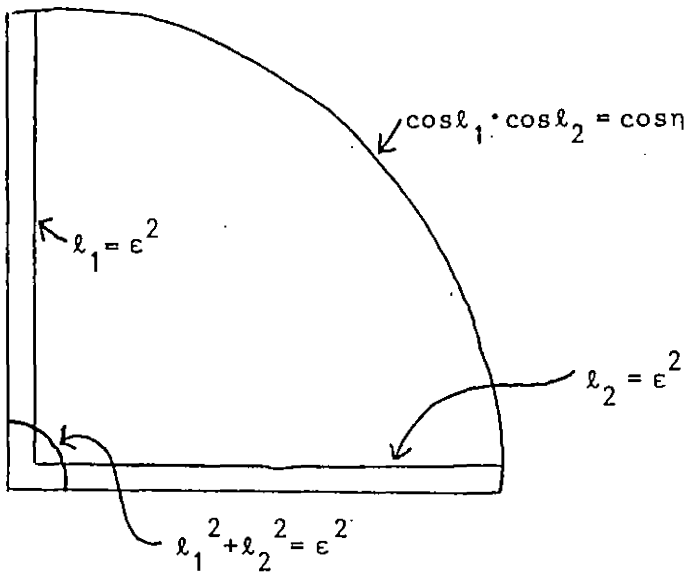


Figure 12

The remaining five examples are obtained with some numerical help based on b) of Lemma 5. Recall that $\underline{\alpha}(s), \overline{\alpha}(s)$ are explicit functions given in Lemma 2. The corresponding $\underline{x}(s), \overline{x}(s)$ are either circles if $\alpha$ = const. or meridians of minimal surfaces of revolution in $S^3$ which are given explicitly in [1,p. 25] in terms of elliptic integrals; of course they are also given as solutions of the Frenet equations (1).

For any $\eta, \ell_1, \ell_2$ we have the bounds $\underline{\alpha}(s), \overline{\alpha}(s)$ of Lemma 2 for the turning angle functions $\alpha(s)$ of $M(\eta, \ell_1, \ell_2)$. Lemma 5b) applied to these explicit bounds and their corresponding Frenet curves gives, through one more integration,

bounds $\underline{\beta}_i \leq \beta_i \leq \overline{\beta}_i$ $(i = 1,2)$, which are shown as boxes in Figure 11. For this last step we rely on numerical integration. The data then show that the continuous center curve of the boxes surrounds the desired $(\beta_1,\beta_2)$-value at such a distance that it is outside of all the error boxes. Since the curve $F_\eta(\ell(s))$ stays in these error boxes, its winding number with respect to $(\beta_1,\beta_2)$ is nonzero . □

Note that beyond existence the above method gives also a certain region R, in $(\ell_1,\ell_2)$-space, in which our desired $(\ell_1,\ell_2)$-value must lie. Combined with our knowledge about the boundary curve of the patch M* (see Lemmas 2 and 5) this allows us to obtain pictures of the stereographic projections of our surfaces, that are qualitatively correct. (See Figs. 3 and 13-16).

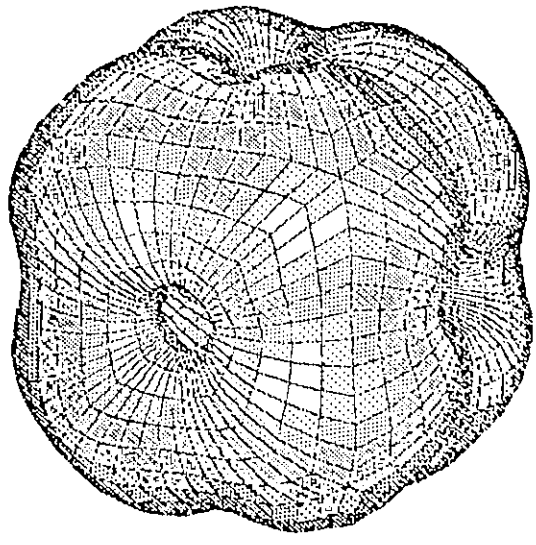

Figure 13

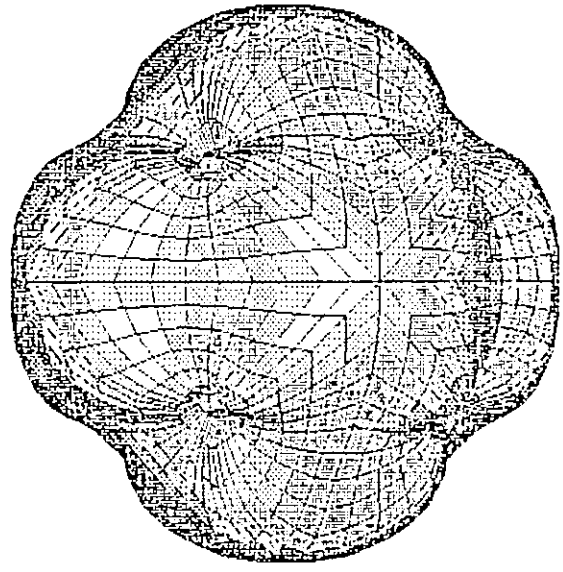

Figure 14

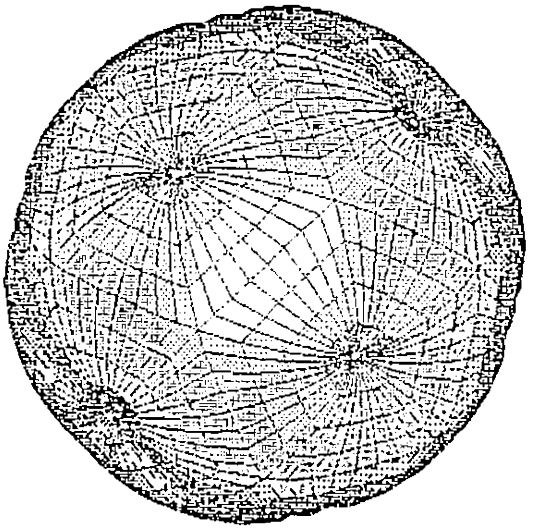

Figure 15

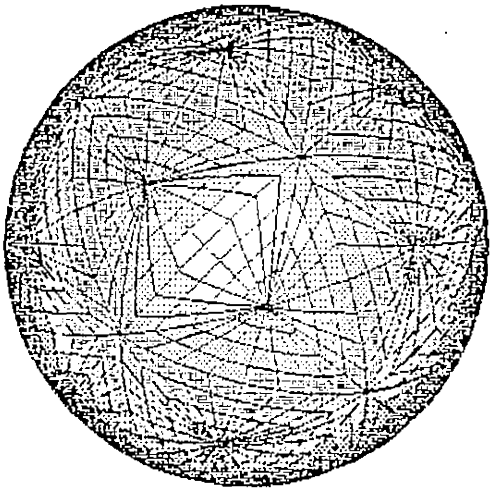

Figure 16

## § 5 Polar varieties, imbeddedness, and volume estimates

Let $M^P$ be the polar variety of $M = M(\eta, \ell_1, \ell_2)$, defined by going a distance $\pi/2$ in the normal direction from $M$. It is again a minimal surface. The polar surface of $M^P$ is again $M$. Let $Q^P$ be its boundary, etc.

Lemma 6. $M^P \subset C(Q^P)$ .

Proof. Let $\Pi$ = plane $(A^P, B^P, C^P)$ = polar plane of $A$ = equator sphere in spherical polar coordinates centered at $A$. Poles of "vertical" (i.e. passing through A) planes in this coordinate system lie in $\Pi$. Since no points of $M = (M^P)^P$ lie in $\Pi$, no tangent planes of $M^P$ are vertical (in particular, $M^P$ does not pass through $A$ or $-A$). Now project $M^P$ to $\Pi$. This gives a local homeomorphism $f: M^P \to \Pi$, and, the boundary curves project $1-1$ to $\Pi$. Therefore, $f$ is a homeomorphism onto the "interior" component of $\Pi - f(Q^P)$. So $M^P \subset f^{-1}(f(M^P))$ (= a spindle with cross section $Q^P$), which is contained in an open hemisphere of $S^3$. The lemma then follows by [4, Th 1].

□

Note. By the same argument as in Lemma 3, $M^P$ is unique and hence it is the Plateau solution of $Q^P$.

Lemma 7. $M^* = M^*(\eta, \ell_1, \ell_2) \subset C(Q^*)$ (resp. $M^{*P} \subset C(Q^{*P})$).

Proof. By [4, Thm. 1], together with the fact that $M$ (resp. $M^P$) is isometric to $M^*$ (resp. $M^{*P}$), it suffices to show that the intrinsic diameter of $M$ (resp. $M^P$) is less than $\pi$. The circumference of $Q$, $\ell_1 + \ell_2 + S_1 + S_2$, is less than $4 \cdot \pi/2$. Two edges of $Q^P$ are $\alpha_1, \alpha_2$, which are both less than $\pi/2$, and since $\eta^P = 180 - \eta$, we also have $S_1^P, S_2^P$ both less than $\pi/2$. Since $M$ and $M^P$ are Plateau discs we have, using two triangles, their areas bounded less than $\pi$. Hence for any piece of them $\int K\,dA \leq \int dA < \pi$. Consequently there are no geodesic loops. Then, the same argument as [2, p. 108] shows that any two points of $M$ (resp. $M^P$) are connected by a unique geodesic in $M$ (resp. $M^P$) shorter than $\pi$, and the lemma follows. □

Lemma 8. For all $(\eta, \beta_1, \beta_2)$ in Table 1, the surface generated by $M^*(\eta, \beta_1, \beta_2)$ is imbedded. (Compare Fig. 1).

Proof. For simplicity, we consider the case $(\pi/3, \pi/2, \pi/3)$ in detail ; the other cases are similar. First, stereographically project so that the plane $\Pi_2^*$ containing $\ell_2^*$ goes to $S^2$ and now work in $\mathbb{R}^3$. $C(Q^{*P}) \cap S^2 = \ell_2^{*P}$. Any "vertical" plane (i.e. vertical to $S^2$) in spherical polar coordinates around $0$ must have its normal on $S^2$. However, by Lemma 7, any interior normal to $M^*$ lies outside $S^2$. Thus $M^*$ is a graph in these coordinates, and the lemma follows. □

It was proved by Lawson that a compact minimal imbedded surface in $S^3$ separates $S^3$ into two diffeomorphic components. The following conjecture is attributed to Lawson [7, p. 692].

Conjecture. Any compact imbedded minimal surface in $S^3$ separates $S^3$ into two components of equal volume.

The surface generated by $M(\pi/3,\pi/2,\pi/5)$ is a counter example.

It suffices to prove $M$ stays within a distance $\pi/2 - D$ ($\approx 23{,}8°$) of its equator of reflections, $E$, where $4D - 2\sin(2D) = \pi$, since this tube around $E$ contains half the volume of $S^3$.

By the analysis in the proof of Lemma 8, the maximum distance from $E$ must occur on $S_1^*$. By Lemma 1, and the remark following equations (4), $S_1^*$ is convex. Hence it suffices to check that $\bar{h} = \pi/2 - \sin^{-1}\{\tan(|S_1^*|)/\tan\phi\}$ is less than $\pi/2 - D$, where $\phi$ is given by $\cos\beta_1 = \sin\eta\cos\phi$.

Finally, by the Theorem, we know $(\ell_1,\ell_2)$ lies within a certain region, $R$, in $(\ell_1,\ell_2)$-space (e.g. here $.54 < \ell_1 < .56, .01 < \ell_2 < 03$). This gives $\max_{(\ell_1,\ell_2)\in R} \bar{h} < 15° < \pi/2 - D$ (the actual value is approximately 7°). (See Fig. 17).

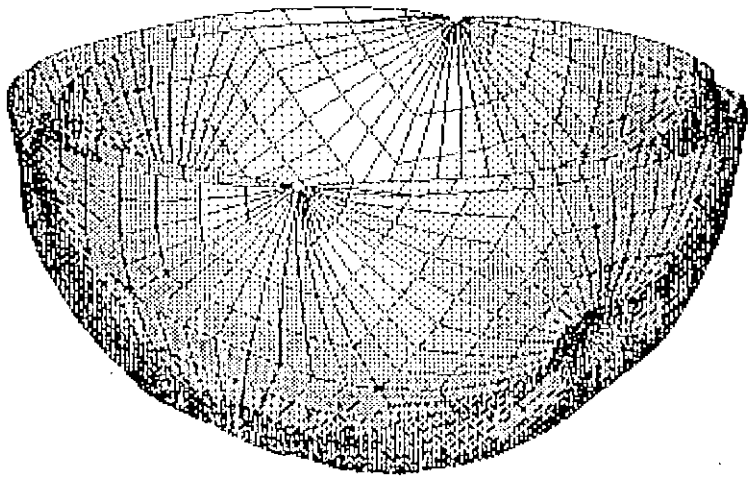

Figure 17

Remark. Computer estimates indicate the area of Lawson's three-hold torus $\xi_{1,3}$ is less than that of the genus three surfaces generated by $M.(\pi/3,\pi/2,\pi/3)$. This lends evidence to the conjecture that stereographic projections of Lawson's n-holed tori $\xi_{1,n}$ are "optimal", in the sense that they are absolute minima of the Willmore integral, $\int H^2 dA$, among all genus $n$ surfaces. Similarly, Lawson's Klein bottle $\tau_{1,2}$ at present is also a candidate to be "optimal". (See Figs. 18 and 19).

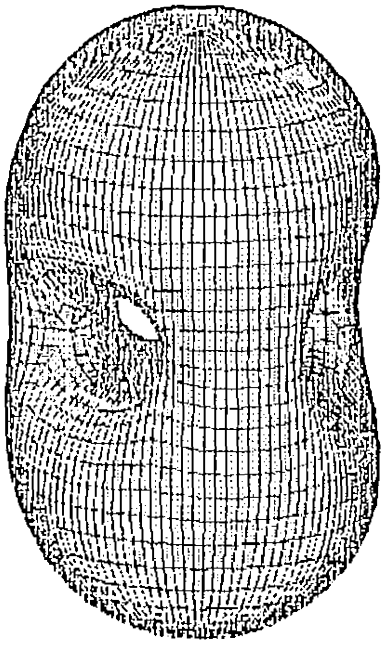

Figure 18

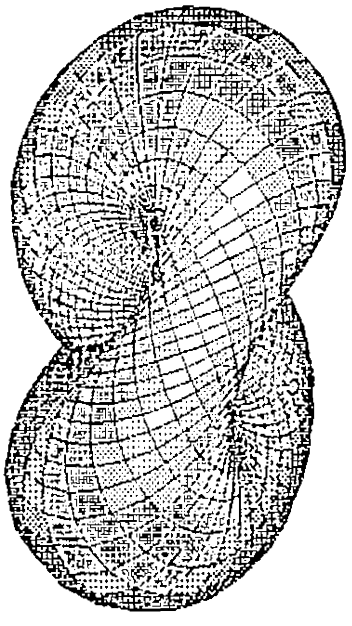

Figure 19

BIBLIOGRAPHY

[1] W. Y. Hsiang and H.B. Lawson, Jr., Minimal submanifolds of low cohomogeneity, J. Diff. Geom., Vol. 5(1971),1-38.

[2] H. Karcher, Schnittort und konvexe Mengen in vollständigen Riemannschen Mannigfaltigkeiten, Math. Annalen, Vol. 177 (1968), 105-121.

[3] H.B. Lawson, Jr., Complete minimal surfaces in $S^3$, Ann. of Math., Vol. 92(1970), 335-374.

[4] ————————, The global behavior of minimal surfaces in $S^n$, Ann. of Math., Vol. 92(1970), 224-237.

[5] W.H. Meeks III, A survey of the geometric results in the classical theory of minimal surfaces, Bol. Soc. Bras. Mat., Vol. 12 No. 1 (1981), 29-86.

[6] B. Smyth, Stationary minimal surfaces with boundary on a simplex, Invent. math. Vol. 76(1984), 411-420.

[7] S.T. Yau, Problem Section, Seminar on differential geometry, Annals of math studies, Vol. 102(1982), 669-706.